

A comprehensive theoretical examination of primary dissociation pathways of formic acid

J. S. Francisco

Citation: *J. Chem. Phys.* **96**, 1167 (1992); doi: 10.1063/1.462204

View online: <http://dx.doi.org/10.1063/1.462204>

View Table of Contents: <http://jcp.aip.org/resource/1/JCPSA6/v96/i2>

Published by the [American Institute of Physics](#).

Additional information on *J. Chem. Phys.*

Journal Homepage: <http://jcp.aip.org/>

Journal Information: http://jcp.aip.org/about/about_the_journal

Top downloads: http://jcp.aip.org/features/most_downloaded

Information for Authors: <http://jcp.aip.org/authors>

ADVERTISEMENT



Goodfellow
metals • ceramics • polymers • composites
70,000 products
450 different materials
small quantities *fast*

www.goodfellowusa.com

A comprehensive theoretical examination of primary dissociation pathways of formic acid

J. S. Francisco

Department of Chemistry, Wayne State University, Detroit, Michigan 48202

(Received 11 July 1991; accepted 30 September 1991)

Primary dissociation pathways have been investigated for formic acid by *ab initio* molecular orbital methods. Reactant, transition state, and products were fully optimized with unrestricted Hartree-Fock and unrestricted second-order Møller-Plesset wave functions. The activation energy for decarboxylation of formic acid ($\text{CO}_2 + \text{H}_2$) is $65.2 \text{ kcal mol}^{-1}$, while that for the dehydration process ($\text{CO} + \text{H}_2\text{O}$) is $63.0 \text{ kcal mol}^{-1}$. These theoretical results suggest that the decarboxylation and dehydration processes are competitive. The activation energy barrier for isomerization of formic acid to yield dihydroxymethylene is $73.7 \text{ kcal mol}^{-1}$ and may be a competitive process. Free radical initiation processes are predicted to be minor.

I. INTRODUCTION

Formic acid is known to decompose by two reaction pathways



with the first process [reaction (1)] being predominant. Blake and Hinshelwood¹ in their studies of the thermal decomposition of formic acid over the temperature range of 709–805 K found rate coefficients for the two processes. However, Benson and O'Neal² later pointed out that possible wall reactions and free radical chain reactions could have obscured the interpretation of the measurements by Blake and Hinshelwood. In a subsequent study, Blake³ re-examined the thermal decomposition of formic acid using both a static and flow system, and reported rate coefficients for the two processes. For the decarboxylation producing CO_2 [reaction (2)] the rate was first-order over the entire temperature range with $k(\text{s}^{-1}) = 10^{12.47} \exp(-48.5 \text{ kcal mol}^{-1}/\text{RT})$. However, for the dehydration [reaction (1)], two rates were reported. At temperatures below 870 K the rate was found to be second order with $k(\text{cm}^3 \text{ mol}^{-1} \text{ s}^{-1}) = 10^{11.44} \exp(-31.7 \text{ kcal mol}^{-1}/\text{RT})$. For temperatures above 950 K, the rate process was found to be of fractional order with $k(\text{s}^{-1}) = 10^{15.39} \exp(-60.5 \text{ kcal mol}^{-1}/\text{RT})$. Samsonov *et al.*⁴ later reported activation energies in the range of 61.7 to 66.0 kcal mol^{-1} for the dehydration reaction which was consistent with the high temperature measurement of Blake.³ Corkum *et al.*⁵ studied the infrared multiphoton decomposition of formic acid initiated by excitation from a pulsed HF laser. The only products observed were CO and H_2O , and an upper limit of 3% was found for the decarboxylation process. It was suggested that the decomposition process resulted from a bimolecular reaction between vibrationally excited formic acid monomers. The lack of isotopic selectivity further supported the argument against a collision free unimolecular decomposition process. Evans *et al.*⁶ examined the infrared multiphoton dissociation of formic acid and measured the products H_2 and CO. Contrary to the study of Corkum, they found the decomposition of formic acid to be isotopically selective. It

was suggested that at low pressures most of the reaction occurred by unimolecular decomposition. At higher pressures, the decomposition process was collisionally assisted. The authors also suggested that the dissociation of formic acid could have primary products that are free radicals. However, their experiments were unable to confirm this possibility. Hsu *et al.*⁷ examined the decomposition of formic acid in a shock tube over the temperature range 1280–2030 K. These authors found that reactions which may involve radicals were not important. Threshold energies for the dehydration and decarboxylation reaction were estimated as 62–65 and 65–68 kcal mol^{-1} for the respective processes. The rates for both processes were second order.

Saito *et al.*⁸ studied the thermal decomposition of formic acid in a shock tube, but unlike the previous study of Hsu *et al.*,⁷ who monitored the concentration profile of CO by using its absorption with a CW CO laser, they followed formic acid and carbon monoxide by its IR emission. A second-order rate coefficient was measured as $k(\text{cm}^3 \text{ mol}^{-1} \text{ s}^{-1}) = 10^{14.32} \exp(-40.4 \text{ kcal mol}^{-1}/\text{RT})$ for the dehydration reaction. This result is inconsistent with the work of Hsu *et al.*⁷ Moreover, in Saito's experiment only small yields of CO_2 was found. This is also in discrepancy with the shock tube results of Hsu *et al.*⁷ *Ab initio* calculations⁸ at the Hartree-Fock level using split-valence basis sets without polarization functions showed that the activation energy for the dehydration process was 67.5 kcal mol^{-1} , while that for the decarboxylation process was 88.9 kcal mol^{-1} ; thus the dehydration reaction was suggested to be the lowest energy channel. The relative energy difference of $\sim 19 \text{ kcal mol}^{-1}$ between the two processes argued in favor of the observations of Saito. However, the calculations did not resolve the discrepancy between the two shock tube studies. Ruelle and co-workers⁹ investigated the mechanism for the two unimolecular decomposition reactions for formic acid using *ab initio* molecular orbital methods. They found that the dehydration reaction was the lowest energy channel with an activation energy of 67.1 kcal mol^{-1} (determined at the MP2/6-311G//HF/6-311G level of theory). The unimolecular decarboxylation reaction was suggested to have an activation energy barrier of 77.6 kcal mol^{-1} (determined

at the MP2/6-31G**//HF/6-31G** level of theory). Ruelle also showed that the activation energy values obtained at the SCF (self-consistent field) level were greatly overestimated. These results did not resolve the discrepancy between the two shock tube studies. In order to explain the second-order dependence of the decarboxylation process and the low activation energy, Ruelle suggested that the decarboxylation was catalytically promoted by water that was produced by the hydration reaction. An activation energy of $48.7 \text{ kcal mol}^{-1}$ was estimated for the process. A later *ab initio* study of Ruelle¹⁰ refined the energetics of the dehydration and decarboxylation processes. In similar work Ruelle¹¹ examined the potential energy surfaces for the dehydration and decarboxylation processes of acetic acid. However, it was later found that these calculations were flawed.¹² Some of the transition states of Ruelle were not true first-order saddle points. This resulted from the fact that the Hessian in internal coordinates was used to determine the nature of the located stationary point instead of a vibrational analysis which is considered the acceptable protocol for characterizing any stationary point. A re-examination of the Ruelle work^{9,10} on formic acid suggests that it too may be similarly flawed. To date only the two concerted unimolecular processes, dehydration and decarboxylation, have been investigated. Moreover, at present there have been no experimental or theoretical investigations into whether free-radical chain reactions may be involved, which as Benson and O'Neal suggested could have obscured the interpretation of the measurements of Blake and Hinshelwood.

In the present study all concerted molecular and bond fission (free-radical initiation) unimolecular dissociation channels are considered for formic acid. These reactions have been studied with significantly more complete inclusion of electron correlation effects. The results further quantify our knowledge of all possible dissociation processes on the potential energy hypersurface of formic acid.

II. COMPUTATION METHODS

Ab initio molecular orbital calculations were performed with the GAUSSIAN 86 system¹³ using split valence (3-21G,¹⁴ 6-31G,¹⁵ and 6-311G¹⁶) basis sets. The 6-31G and 6-311G basis sets were also supplemented with polarization functions¹² and diffuse functions.¹⁷ All equilibrium geometries and transition state structures were fully optimized using analytical gradient methods.¹⁸ In optimizations performed with second-order Møller-Plesset perturbation theory all electrons were unfrozen. Higher order electron correlation was estimated by Møller-Plesset perturbation theory¹⁹ up to fourth order, including all single, double, quadruple, and triplet excitations (MP4SDTQ, frozen core). Vibrational frequencies and zero-point energies were obtained from analytical second derivatives²⁰ calculated at the HF/3-21G level of theory using the HF/3-21G optimized geometry.

A. Molecular structures

1. Reactant and products

The optimized geometries for all reactants and products are listed in Table I. Although the geometries for some of the reactants and products have been published previously, they are reproduced here to facilitate comparison with other structures. Comparison with the available experimental structures indicated that the overall agreement is good: $\pm 0.008 \text{ \AA}$ (rms) for bond lengths and $\pm 3^\circ$ (rms) for angles at the UMP2/6-311G** level of theory

Calculated structural features for *trans*-formic acid are compared with values derived from microwave experiments.^{21,22} The OH and CH bond distances at the UMP2/6-311G* level are in good agreement with the experimental values. The C-O bond length seems intermediate between those determined from experiment (1.312^{21} and 1.36 \AA^{22}). There is reasonable agreement between UMP2/6-311G** calculated angles and experiment; differences are generally less than $\pm 2^\circ$ (rms). For example, the calculated HOC angle of 105.6° is in good agreement with the experimental value of 105.0° reported by Karle and Karle²² and overestimates the experimental value reported Lerner *et al.*²¹ by 2° . Likewise, for the OC=O angle the calculated value of 125.2° agrees well with the experimental determinations.

Equilibrium geometries for hydroxyformyl radical [C(O)OH] in its doublet ground state are given in Table I. A comparison of CO and HO bond lengths with that in formic acid reveal that the structure of C(O)OH radicals mimic that of formic acid quite well. The major structural difference is in the OC=O angle, which is larger for the radical than in formic acid. It is interesting that the *trans* structure for hydroxyformyl radical is found to be $0.2 \text{ kcal mol}^{-1}$ lower in energy than the *cis* structure at the UHF/6-311G* level of theory. The small energy differences between the two structures at the Hartree-Fock level cannot yield a conformational preference for hydroxyformyl radical unambiguously. However, at the correlated levels of theory the *cis* structure is more stable. The stabilization energy is $1.6 \text{ kcal mol}^{-1}$ at the UMP2/6-311G** level and $2.6 \text{ kcal mol}^{-1}$ at the PMP4/6-311++G**//UMP2/6-311G** level of theory. Consequently, the *cis* conformation of C(O)OH radical is the more stable structure by $2.6 \text{ kcal mol}^{-1}$. This is in reasonable agreement with the CI work on hydroxyformyl radical by McLean and Ellinger.²³ They find a stabilization energy of $3.3 \text{ kcal mol}^{-1}$.

The geometry for the dihydroxymethylene in its singlet ground state is given in Table I. The results for *cis* and *trans* structures are interesting. The CO bond lengths in the *cis* structure optimized to equal lengths (i.e., CO = 1.324 \AA); however, the CO bond lengths in the *trans* structure were found to be unequal in length (i.e., CO = 1.228 \AA and CO' = 1.310 \AA). Further comparison with the *cis* species show that any steric crowding in the *trans* structure is relieved by increasing the CO and HOC angles. At the UHF/3-21G level the *trans* structure is preferred, and at the UHF/6-311G* level the *cis* structure is preferred over the *trans* by $0.1 \text{ kcal mol}^{-1}$. However, correlation effects are important for these species. Large basis sets and higher cor-

TABLE I. Optimized ground state geometries for species involved in HC(O)OH dissociation. (Bond distances in Å, angles in degrees).

Species	Coordinate	UHF/3-21G	UHF/6-31G*	UMP2/6-31G*	UMP2/6-311G**	Expt.	
H ₂	H-H	0.735	0.730	0.738	0.735		
OH	O-H	0.986	0.958	0.979	0.966	0.970	
CO	C-O	1.129	1.114	1.150	1.138	1.128	
CO ₂	C-O	1.156	1.143	1.179	1.168		
H ₂ O	O-H	0.967	0.947	0.969	0.952	0.958	
	HOH	107.6	105.6	104.0	102.5	104.5	
HCO	C-H	1.095	1.105	1.124	1.123	1.125	
	C-O	1.180	1.159	1.191	1.182	1.175	
	HCO	129.0	126.3	123.4	123.8	125.0	
H ₂ CO	C-H	1.083	1.092	1.104	1.106	1.120	
	C=O	1.207	1.184	1.220	1.210	1.210	
	HCO	122.5	122.1	122.8	122.2	118.0	
HCO ₂	C-H	1.080	1.089	1.107	1.109		
	CO	1.193	1.177	1.210	1.200		
	CO'	1.366	1.324	1.338	1.329		
	HCO	126.6	126.2	126.6	126.8		
	OCO'	124.7	124.6	125.5	126.1		
HO- \ddot{C} -OH, <i>trans</i>	C-O	1.357	1.321	1.349	1.338		
	C-O'	1.327	1.300	1.319	1.310		
	H-O	0.963	0.948	0.973	0.961		
	H-O'	0.976	0.958	0.989	0.976		
	HOC	112.8	112.2	106.5	105.7		
	OCO'	105.7	107.2	106.2	107.2		
	HO'C	114.5	108.9	110.3	109.3		
	HO'CO	0.0	0.0	0.0	0.0		
	HOCO'	180.0	180.0	180.0	180.0		
HO- \ddot{C} -OH, <i>cis</i>	C-O	1.337	1.309	1.334	1.324		
	C-O'	1.337	1.309	1.334	1.324		
	H-O	0.963	0.947	0.973	0.960		
	H-O'	0.963	0.947	0.973	0.960		
	HOC	111.6	108.1	105.4	104.5		
	OCO'	105.2	105.5	104.0	104.9		
	HO'C	111.6	108.1	105.4	104.5		
	HO'CO	180.0	180.0	180.0	180.0		
	HOCO'	180.0	180.0	180.0	180.0		
C(O)OH, <i>trans</i>	C=O	1.184	1.167	1.198	1.187		
	C-O'	1.335	1.311	1.377	1.331		
	H-O'	0.975	0.975	0.984	0.971		
	O=CO'	131.4	130.4	130.2	130.5		
	HO'C	115.1	109.9	108.1	107.0		
	HO'CO	0.0	0.0	0.0	0.0		
C(O)OH, <i>cis</i>	C=O	1.176	1.162	1.194	1.183		
	C-O'	1.351	1.322	1.351	1.344		
	H-O'	0.966	0.949	0.975	0.962		
	O=CO'	128.8	128.2	126.6	127.2		
	HO'C	113.3	110.4	107.5	106.3		
	HO'CO	180.0	180.0	180.0	180.0		
HC(O)OH, <i>trans</i>	C=O	1.198	1.182	1.213	1.202	1.245 ^a	1.23 ^b
	C-O	1.351	1.323	1.351	1.346	1.312	1.36
	H-O	0.970	0.954	0.980	0.967	0.95	0.97
	C-H	1.074	1.083	1.096	1.097	1.085	1.09
	HC=O	125.8	124.7	125.4	125.6
	OC=O	124.6	124.9	125.1	125.2	124.3	122.4
	HOC	112.7	108.7	106.1	105.6	107.8	105.0
	HOC=O	0.0	0.0	0.0	0.0	0.0	0.0
HC(O)OH, <i>cis</i>	C=O	1.192	1.176	1.206	1.196		
	C-O	1.354	1.328	1.356	1.352		
	H-O	0.964	0.948	0.974	0.962		
	C-H	1.082	1.090	1.104	1.104		
	HC=O	123.6	123.1	123.8	124.0		
	OC=O	122.6	123.0	122.5	122.8		
	HOC	114.8	111.6	109.1	107.8		
	HOC=O	180.0	180.0	180.0	180.0		

^a Reference 21.^b Reference 22.

relation effects consistently predict *cis*-dihydroxymethylene to be more stable than its *trans* conformation. At the PMP4/6-311 + + G**//UMP2/6-311G** level of theory the stabilization energy is 1.4 kcal mol⁻¹.

2. Transition state structures

The calculated transition structure for the decarboxylation process is shown in Fig. 1(a). The full geometries are given in Table II. This pathway has a tight four-centered transition state. The reverse of this reaction is the addition of molecular hydrogen to CO₂. The breaking of the CH and OH bonds occurs unsymmetrically, leading in a rather distorted four-centered transition state. Similar distortions²⁴ are found in transition states for 1, 2-hydrogen elimination in C₂H₆.

The structure for the 1, 2-hydrogen shift transition state for the dehydration process [shown in Fig. 1(b)] may be compared with the 6-31G** SCF result of Ruelle *et al.*⁹ Ruelle suggested that the transition state for the process is planar. In this work, the transition state is not planar. The torsion angle between the hydrogen on the hydroxyl group and the plane of the OCO groups is 74.8°. Moreover, as in many 1, 2-hydrogen shift transition structures,²⁵ the hydrogen is quite close both to the atom it is leaving (in this case C) and the one to which it is transferring (in this case O). The CH distance of 1.153 (UMP2/6-311G**) is shorter than the OH' distance of 1.407 Å (UMP2/6-311G**). The CO bond length of 1.821 Å is 0.472 Å longer than in formic acid which suggests that it is nearly broken.

The transition state structure for the isomerization of formic acid to dihydroxymethylene is shown in Fig. 1(c). The CH bond in the transition state only lengthens by 12% relative to formic acid at the UMP2/6-311G** level of theory, while the newly formed OH bond is 27% elongated from that in the product dihydroxymethylene. Comparing the CH and CO bond lengths, it appears that the leaving hydrogen is closer to the transferring oxygen than it is to the leaving carbon. This type of transfer for the 1, 2-hydrogen shift is consistent with those observed for other systems.²⁵

B. Vibrational frequencies

The HF/3-21G harmonic frequencies for formic acid and its various transition states are listed in Table III. Formic acid is a planar molecular possessing C_s symmetry and its vibrations span the representation

$$\Gamma = 7a' + 2a'' \quad (3)$$

All vibrations in this representation are infrared and Raman active. Calculated frequencies of formic acid compared to experimental ones²⁶ are overestimated by ~10%–15% owing to the use of harmonic approximation, the truncation of the basis set, and to the neglect of electron correlation in the HF/3-21G frequency calculation.²⁰ Nevertheless, the calculated frequencies appear in the correct order. The largest errors are primarily in OH and CH stretching frequencies, while the lower frequency (deformation, rocks, and torsions) modes show better agreement with experiment.

More importantly, the harmonic vibrational frequencies for the transition state structures verify their nature as

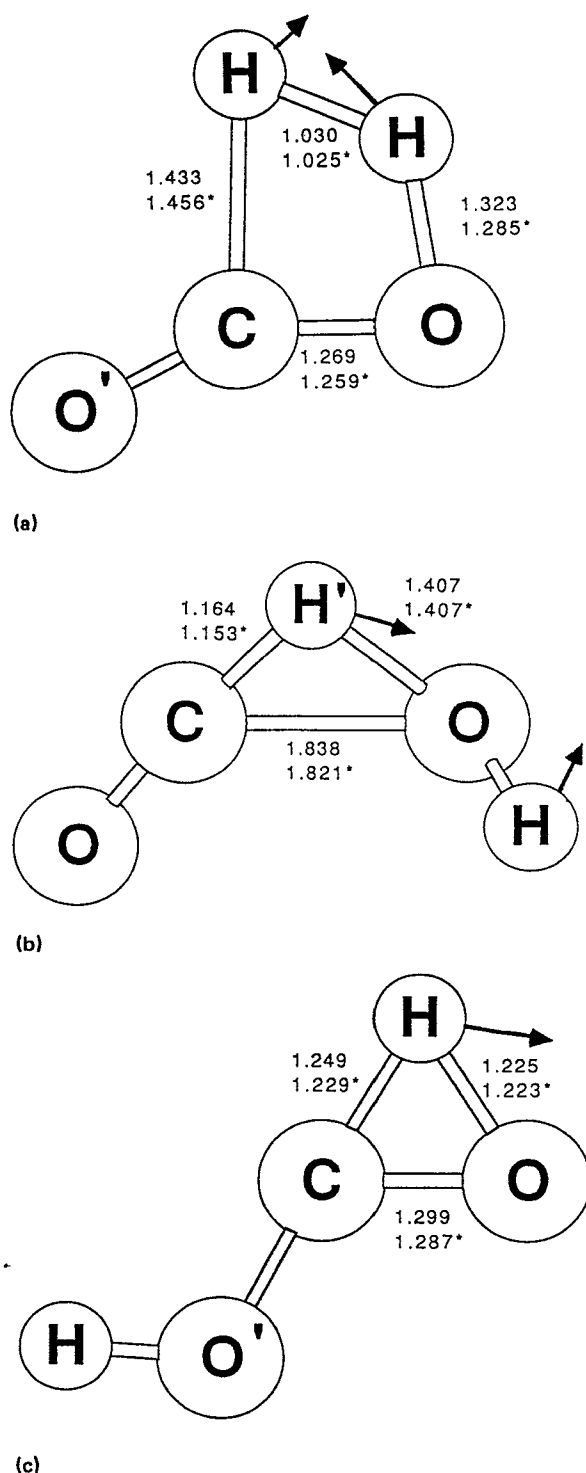


FIG. 1. Transition states and transition vectors for formic acid unimolecular dissociations (MP2/6-31G* optimized—no asterisk; MP2/6-311G** optimized—asterisk; see Table II for the complete list of geometric parameters): (a) the predicted structure for the decarboxylation reaction; (b) the predicted structure for the dehydration reactions; (c) the predicted structure for the 1,2-hydrogen shift isomerization reaction.

first order saddle points (Hessian index 1) with exactly one imaginary vibrational frequency. For the decarboxylation reaction, the imaginary frequency is quite large (2924i cm⁻¹). The transition vector consists mainly of a CH stretch in the OCH plane mixed with the OH stretch in the

TABLE II. Optimized transition state geometries for species involved in HC(O)OH dissociation (bond distances in Å, bond angles in degrees).

Reaction	Coordinate	UHF/3-21G	UHF/6-31G*	UMP2/6-31G*	UMP2/6-311G**	
HC(O)OH → CO ₂ + H ₂	CO	1.266	1.236	1.269	1.259	
	CO'	1.144	1.143	1.184	1.172	
	CH	1.658	1.486	1.433	1.456	
	HO	1.229	1.257	1.323	1.285	
	HH	1.123	1.044	1.030	1.025	
	HCO	88.4	96.0	99.7	98.1	
	HOC	81.2	72.2	67.9	68.5	
	O'CO	152.8	149.7	146.4	147.9	
	HOCH	0.0	0.0	0.0	0.0	
	HC(O)OH → CO + H ₂ O	CO	1.763	1.856	1.838	1.821
		CO'	1.144	1.122	1.167	1.156
CH'		1.190	1.151	1.164	1.153	
H'O		1.315	1.396	1.407	1.407	
HO		0.973	0.952	0.981	0.968	
H'CO		48.2	48.7	49.9	50.6	
H'OC		42.4	38.3	39.3	39.3	
O'CO		124.5	123.8	121.8	121.8	
H'OH		140.1	122.2	110.8	111.0	
HOCO		57.9	72.4	76.1	74.8	
HC(O)OH → HO-C-OH		CO	1.286	1.252	1.299	1.287
	CO'	1.325	1.306	1.339	1.331	
	CH	1.229	1.208	1.249	1.229	
	HO	1.254	1.224	1.225	1.223	
	HO'	0.965	0.949	0.975	0.963	
	HCO	59.8	59.6	57.4	58.1	
	HOC	57.9	58.4	59.3	58.6	
	OCO'	118.3	117.5	114.4	115.6	
	HO'C	113.9	109.9	107.1	105.9	
	HO'CO	180.0	180.0	180.0	180.0	
	HOCO'	180.0	180.0	180.0	180.0	
HC(O)OH, <i>trans</i> → HC(O)OH, <i>cis</i>	C=O	1.192	1.174	1.206	1.196	
	C-O	1.375	1.351	1.379	1.376	
	H-O	0.968	0.950	0.973	0.961	
	C-H	1.079	1.087	1.101	1.101	
	HC=O	123.4	123.0	123.3	123.5	
	OC=O	123.7	123.9	124.0	124.0	
	HOC	115.5	112.0	110.3	107.8	
	HOC=O	99.8	96.0	95.3	94.3	

TABLE III. Vibrational frequencies (cm⁻¹) and zero point energies (kcal mol⁻¹) for species involved in the HC(O)OH dissociation.

Reactants & products	Vibrational frequencies (UHF/3-21G)	Zero point energy
H ₂	4656	6.7
OH	3609	5.2
CO	2314	3.3
CO ₂	659, 659, 1427, 2463	7.4
H ₂ O	1799, 3183, 3947	13.7
HCO	1239, 1945, 2967	8.8
H ₂ CO	1337, 1378, 1693, 1916, 3163, 3234	18.2
<i>trans</i> HO-C-OH	627, 707, 841, 1154, 1198, 1381, 1515, 3741, 3938	21.6
<i>cis</i> HO-C-OH	652, 696, 745, 1165, 1186, 1442, 1488, 3927, 3927	21.8
<i>trans</i> C(O)OH	568, 643, 1115, 1396, 1967, 3755	13.5
<i>cis</i> C(O)OH	480, 665, 1107, 1274, 2030, 3894	13.5
<i>trans</i> HC(O)OH	669, 677, 1180, 1194, 1423, 1552, 1939, 3329, 3859	22.6
<i>cis</i> HC(O)OH	438, 709, 1186, 1196, 1300, 1598, 1999, 3215, 3907	22.2
HC(O)O	636, 1075, 1137, 1501, 1909, 3244	13.6
HC(O)OH → [CO ₂ + H ₂] [‡]	2924 <i>i</i> , 561, 707, 765, 1221, 1227, 1674, 2033, 2318	15.0
HC(O)OH → [CO + H ₂ O] [‡]	2035 <i>i</i> , 266, 420, 604, 900, 1147, 2012, 2583, 3783	16.7
HC(O)OH → [HO-C-OH] [‡]	2550 <i>i</i> , 296, 600, 655, 1219, 1276, 1633, 2696, 3909	17.6
HC(O)OH → [HC(O)OH] _{<i>t,c</i>} [‡]	524 <i>i</i> , 723, 1002, 1170, 1315, 1581, 1969, 3265, 3861	21.3

TABLE IV. Total energies (hartrees) for reactants, products, and transition states for HC(O)OH dissociation.

Species	UHF/3-21G	UHF/6-31G*	UMP2/6-31G*	UMP2/6-311G**	UMP4/6-311 + + G**// UMP2/6-311G**	PMP4/6-311 + + G**// UMP2/6-311G**
Reactants and products						
H	-0.496 20	-0.498 23	-0.498 23	-0.499 81	-0.499 81	-0.499 81
O(¹ D)	-74.267 45	-74.656 60	-74.772 01	-74.827 28	-74.836 34	-74.836 34
H ₂	-1.122 96	-1.126 83	-1.160 27	-1.167 76	-1.167 76	-1.167 76
OH	-74.970 23	-75.382 28	-75.523 21	-75.591 40	-75.595 55	-75.596 56
CO	-112.093 30	-112.737 88	-113.028 18	-113.111 42	-113.102 13	-113.102 13
CO ₂	-186.561 26	-187.634 18	-188.118 36	-188.255 33	-188.232 46	-188.232 46
H ₂ O	-75.585 96	-76.010 75	-76.199 24	-76.282 89	-76.287 21	-76.287 21
HCO	-112.603 80	-113.247 66	-113.540 33	-113.630 60	-113.624 69	-113.626 94
H ₂ CO	-113.221 82	-113.866 33	-114.174 96	-114.272 43	-114.269 40	-114.269 40
HCO ₂	-187.072 90	-188.130 12	-188.573 07	-188.714 84	-188.705 24	-188.706 73
HO-C-OH, <i>trans</i>	-187.641 19	-188.692 12	-189.170 94	-189.334 89	-189.325 65	-189.325 65
HO-C-OH, <i>cis</i>	-187.637 65	-188.692 32	-189.170 44	-189.336 01	-189.328 27	-189.328 27
C(O)OH, <i>trans</i>	-187.066 81	-188.127 50	-188.597 59	-188.746 03	-188.730 26	-188.731 56
C(O)OH, <i>cis</i>	-187.067 17	-188.127 13	-188.599 32	-188.748 59	-188.734 28	-188.735 68
HC(O)OH, <i>trans</i>	-187.700 20	-188.762 31	-188.251 87	-189.408 04	-189.394 77	-189.394 77
HC(O)OH, <i>cis</i>	-187.688 68	-188.752 55	-189.242 48	-189.399 49	-189.387 61	-189.387 61
Transition states						
HC(O)OH, <i>trans</i>						
-HC(O)OH, <i>cis</i>	-187.680 96	-188.740 76	-189.228 34	-189.385 87	-189.374 13	-189.374 13
HC(O)OH → CO ₂ + H ₂	-187.530 58	-188.603 24	-189.123 89	-189.291 23	-189.278 83	-189.278 83
HC(O)OH → CO + H ₂ O	-187.565 14	-188.611 94	-189.128 58	-189.291 04	-189.285 02	-189.285 02
HC(O)OH → HO-C-OH	-187.532 66	-188.740 76	-189.113 13	-189.277 85	-189.269 42	-189.269 42

COH plane. There is also mixing of these modes with the OH bending mode, which is to be expected considering the highly strained four-center structure. The remaining modes, for the most part, lie between the frequencies of the reactants and products. The imaginary frequency for the dehydration reaction is also large ($2035i\text{ cm}^{-1}$), and is due to the involvement of the CH and OCH bend motion along the reaction coordinate at the transition state. Judging from the transition vectors considerable motion in the resulting products may result in the bending mode of water. In the 1, 2-hydrogen shift transition state connecting formic acid to dihydroxymethylene, the value of the imaginary frequency is $2550i\text{ cm}^{-1}$. The motion is dominated by the hydrogen transfer through the CH stretch. Most of the remaining modes of this structure mimic those of the product with the exception of one very low frequency mode (296 cm^{-1}) which corresponds to HOCO torsion mixed with the OC·H·O twist- ing motion.

C. Relative energies and comparison with experiment

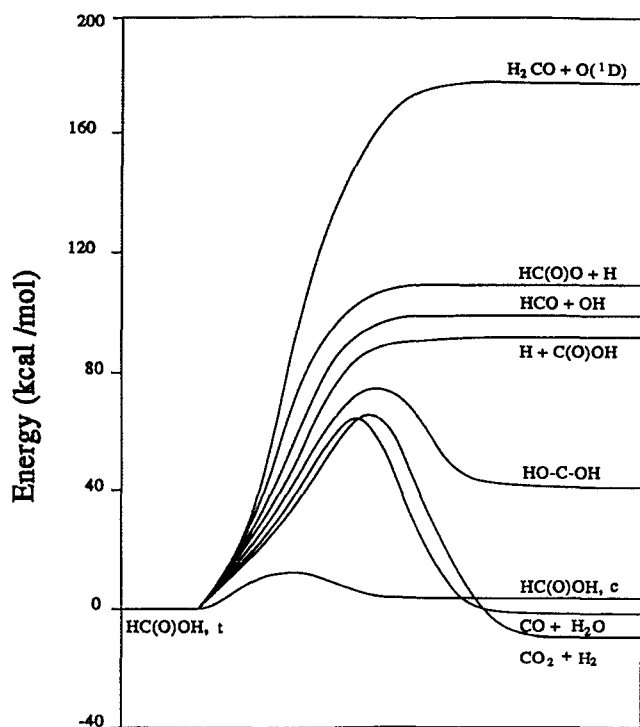
Tables IV and V present the total and relative energies for reactants, products and transition states for formic acid dissociations. The potential energy surface is summarized in Fig. 2. Considering firstly the *cis*-*trans* isomerization of formic acid, the higher levels of theory show good convergence for the energy difference between *trans* and *cis*-formic acid ($\Delta E = 6.1\text{--}4.5\text{ kcal mol}^{-1}$) and *trans*-formic acid and the rotational transition state ($\Delta E = 14.8\text{--}13.0\text{ kcal mol}^{-1}$). The average change in the ΔE is 1.7 kcal mol^{-1} . Inclusion of zero-point energy, reduces the rotational barrier for *trans*-*cis* isomerization of formic acid to $11.7\text{ kcal mol}^{-1}$ and the heat of reaction, $\Delta H_{0,r}$, to 4.1 kcal mol^{-1} . The present work

which uses quite flexible basis sets and higher order electron correlation is quite reasonable when compared with previous theoretical results.²⁷⁻³⁰ The difference in previous theoretical determinations and the present is 1.6 kcal mol^{-1} at most. There have been several experimental determinations of the rotational barrier.^{21,31,32} The values range from $17\text{--}13.4\text{ kcal mol}^{-1}$. Miyazawa and Pitzer³¹ determined the barrier to be $10.9\text{ kcal mol}^{-1}$, which is in good agreement with the present results (see Table VI). Moreover, the heat of reaction calculated in the present work (4.1 kcal mol^{-1}) compares well with the experimental values of 4.0 kcal mol^{-1} reported by Lide³³ and $4.09\text{ kcal mol}^{-1}$ reported by Bjarnov and Hocking.³⁴ Goddard, Yamaguchi and Schaefer³⁵ predicted the energy difference between *trans* and *cis*-formic acid to be 4 kcal mol^{-1} and a barrier to internal rotation of 12 kcal mol^{-1} . Their results are consistent with the present work.

The effect of basis set and electron correlation on the activation energy for the molecular processes are quite significant, e.g., changes of $\pm 20\text{ kcal mol}^{-1}$, upon going from the smaller (3-21G) to larger basis set (6-311G**). For the decarboxylation reaction, both the addition of polarization functions and correlation effects play a major role in lowering the activation energy. However, the largest change ($19.5\text{ kcal mol}^{-1}$) comes from inclusion of electron correlation in going from HF/6-31G to MP2/6-31G*. A large basis set, 6-311G** and the addition of MP2 correlation lead to a 7 kcal mol^{-1} reduction in the energy. Making the basis set more flexible by the addition of diffuse functions to all the atoms and inclusion of higher order electron correlation (MP4SDTQ) only produces a modest change in the barrier from that determined at the MP2/6-311G** level of theory ($\sim 0.5\text{ kcal mol}^{-1}$). Corrections for zero-point vibrational

TABLE V. Heats of reaction and activation energies (kcal mol^{-1}) for HC(O)OH dissociation pathways.

	UHF/3-21G	UHF/6-31G*	UMP2/6-31G*	UMP2/6-311G**	UMP4/ 6-311 + + G***// UMP2/6-311**	PMP4/ 6-311 + + G***// UMP2/6-311G**	ΔZPE	PMP4/6-311 + + G***// UMP2/6-311G** + ΔZPE
HC(O)OH, trans $\rightarrow \text{HC(O)OH, cis}$	7.2	6.1	5.9	5.4	4.5	4.5	-0.4	4.1
$[\text{HC(O)OH, trans}$ $\rightarrow \text{HC(O)OH, cis}]^\ddagger$	12.1	13.5	14.8	13.9	13.0	13.0	-1.3	11.7
HC(O)OH $\rightarrow \text{CO}_2 + \text{H}_2$	10.0	0.8	-16.8	-9.4	-3.4	-3.4	-8.5	-11.9
$[\text{HC(O)OH}$ $\rightarrow \text{CO}_2 + \text{H}_2]^\ddagger$	106.4	99.8	80.3	73.3	72.8	72.8	-7.6	65.2
HC(O)OH $\rightarrow \text{CO} + \text{H}_2\text{O}$	13.1	8.6	15.3	8.6	3.4	3.4	-5.6	-2.2
$[\text{HC(O)OH}$ $\rightarrow \text{CO} + \text{H}_2\text{O}]^\ddagger$	84.7	94.4	77.4	73.4	68.9	68.9	-5.9	63.0
HC(O)OH $\rightarrow \text{HO}-\ddot{\text{C}}-\text{OH}$	37.0	44.0	50.8	45.9	41.7	41.7	-1.0	40.7
$[\text{HC(O)OH}$ $\rightarrow \text{HO}-\ddot{\text{C}}-\text{OH}]^\ddagger$	105.1	101.6	87.1	81.7	78.7	78.7	-5.0	73.7
HC(O)OH $\rightarrow \text{HCO} + \text{OH}$	79.2	83.1	118.2	116.7	109.5	107.5	-8.6	98.9
HC(O)OH $\rightarrow \text{H} + \text{C(O)OH}$	85.9	85.9	96.8	100.2	100.8	99.9	-9.1	90.8
HC(O)OH $\rightarrow \text{HC(O)O} + \text{H}$	82.3	84.1	113.3	121.3	119.1	118.1	-9.0	109.1
HC(O)OH $\rightarrow \text{H}_2\text{CO} + \text{O}(^1\text{D})$	132.4	150.2	191.3	193.5	181.4	181.4	-4.4	177.0

FIG. 2. Relative energies in kcal mol^{-1} for the formic acid potential energy surface.

effects lead to an activation energy barrier of $65.2 \text{ kcal mol}^{-1}$ for the decarboxylation reaction. Ruelle⁹ estimated the activation energy for this reaction to be $77.61 \text{ kcal mol}^{-1}$ at the MP2/6-31G**//HF/6-31G** level of theory. Later, he reestimated the activation energy to be $75.97 \text{ kcal mol}^{-1}$ at the MP4SDTQ/6-31G**//MP2/6-31G* level of theory¹⁰ but did not include zero-point energy corrections. Nevertheless, this work suggests that geometry optimization with large flexible basis sets and correlated wave functions is necessary for describing the energetics of the decarboxylation reaction. The extensive calculation of Goddard, Yamaguchi, and Schaefer³⁵ using, TZ + 2P CCSD//DZ + P CCSD with estimation of the triplet contributions and inclusion of zero-point energy yields an estimate of the activation energy of 71 kcal mol^{-1} which is consistent with the present result.

Blake³ estimated the threshold energy for the decarboxylation reaction to be $48.5 \text{ kcal mol}^{-1}$. In shock tube studies of Saito,⁸ an estimate for the energy threshold of $60.6 \text{ kcal mol}^{-1}$ was determined using low level *ab initio* results coupled with RRKM theory modeling of the CO_2 yields. The experimental estimate of the threshold energy ($65\text{--}68 \text{ kcal mol}^{-1}$) by Hsu *et al.*⁷ and by Saito⁸ is, however, consistent with the present theoretical result of $65.2 \text{ kcal mol}^{-1}$ for the decarboxylation reaction. This suggests that results of Blake³ may have resulted from other processes.

The dehydration reaction constitutes the main channel

TABLE VI. Comparison of experimental and theoretical activation energies (kcal mol⁻¹).

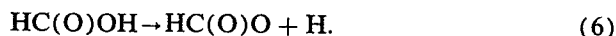
Reaction	Method	Activation energy	Reference
HC(O)OH, <i>trans</i> → HC(O)OH, <i>cis</i>	Theory	12.2	27
		9.6	28
		11.2	This work
		12	35
	Experiment	17	21
		10.9	31
		13.4	32
HC(O)OH → CO ₂ + H ₂	Theory	77.61	9
		75.97	10
		65.2	This work
		71	35
	Experiment	48.5	3
		65–68	7
		60.6	8
		67.1	9
HC(O)OH → CO + H ₂ O	Theory	78.71	10
		63.0	This work
		68	35
		60.5	3
	Experiment	61.7–66.0	4
		62–65	7
		40.4	8

observed in the pyrolysis of formic acid; from a theoretical point of view, changes in the activation energy in going from Hartree–Fock to MP2 levels of theory are quite similar to those for the decarboxylation reaction. The resulting activation energy for the dehydration process calculated at the PMP4/6–311 + + G**//UMP2/6–311G** level of theory with inclusion of zero-point energy correction is 63.0 kcal mol⁻¹. This is quite similar to the estimate of Ruelle which is 67.1 kcal mol⁻¹ and that of Goddard, Yamaguchi, and Schaefer³⁵ of 68 kcal mol⁻¹. Compared with the experimental results the calculated ones agree well with those of Blake,³ Hsu,⁷ and Samsonov⁴ (see Table VI). When comparing activation energies for the dehydration versus the decarboxylation process it should be noted that the present theoretical results are also consistent with the general observation that the dehydration reaction dominates. However, the decarboxylation process should be competitive which suggests that yields of CO₂ and CO should be nearly similar. Hsu *et al.*⁷ did find about the same yields of CO₂ and CO in their study which is consistent with the implications from the present work. However, in the experiment of Saito *et al.*⁸ only a small yield of CO₂ was observed, which caused considerable discrepancy between the two shock tube results and also contributed to the estimation of the small energy threshold of 40.4 kcal mol⁻¹ for the dehydration process. The low CO yield observed by Saito *et al.* may have been due to efficient quenching of the ir emission from CO by formic acid which would lead to the observance of low signals for CO. This coupled with the analysis of the initial part of the CO profile may have led to errors in the rate coefficient determination.

In the studies of Ruelle^{9,10} only dehydration and decarboxylation processes were considered for the unimolecular decomposition of formic acid. A question raised here was

could the CO or CO₂ yields measured in the experiment come from other sources. One such source is from the decomposition of dihydroxymethylene. However, the key question is whether the 1, 2-hydrogen shift is more competitive than the dehydration and decarboxylation process. Earlier *ab initio* studies^{36,37} of the 1, 2-hydrogen shift process suggested that the barrier from *cis*-formic acid to the dihydroxymethylene is ~80 kcal mol⁻¹. The activation energy barrier for the 1,2-hydrogen shift isomerization process calculated in the present study is 73.7 kcal mol⁻¹. It is 10.7 and 8.5 kcal mol⁻¹ above the dehydration and decarboxylation processes, respectively. It is not the lowest unimolecular decomposition channel. However, at shock tube temperatures of 1370–2000 K, this reaction could be competitive. Consequently, decomposition of the dihydroxymethylene in the shock tube could be another source of CO or CO₂.

Following the suggestion of Benson and O'Neal² that free radical chain reactions could have complicated⁹ the interpretation of Blake and Hinshelwood's measurements, the energetics of these processes have been considered in this work. Probable radical processes are



If these reactions are important initiation processes, the decomposition of the HCO could be a source of CO and the radicals C(O)OH and HC(O)O could be a source of CO₂. The lowest energy radical initiation process is reaction (5). Its CH bond dissociation energy for this process is 90.8 kcal mol⁻¹. Cleavage of the CO bond requires an additional 8.1 kcal mol⁻¹ above the CH bond dissociation energy. The least favorable pathway is cleavage of the OH bond to yield

HC(O)O and hydrogen atoms. The bond dissociation energy is $109.1 \text{ kcal mol}^{-1}$. Nevertheless, the present results suggest that contributions to the unimolecular decomposition of formic acid by free radical initiated processes are small. Consequently, in shock tube and thermal pyrolysis studies, these processes are unimportant.

III. CONCLUSIONS

The major conclusions of this work may be summarized briefly as follows:

(1) The activation energies for dehydration and decarboxylation processes are 63.0 and $65.2 \text{ kcal mol}^{-1}$. These results are consistent with experimental results of Hsu *et al.*

(2) The 1, 2-hydrogen shift isomerization process to yield dihydroxymethylene requires an activation energy of $73.7 \text{ kcal mol}^{-1}$.

(3) Radical chain processes are suggested to be minor.

- ¹ P. G. Blake and C. Hinshelwood, *Proc. R. Soc. London Ser. A* **255**, 444 (1960).
- ² S. W. Benson and H. E. O'Neal, *Kinetic Data on Gas Phase Unimolecular Reaction*, Natl. Stand. Ref. Data Ser. Natl. Bur. Stand. 21 (US. GPO, Washington, D.C., 1970), p. 111.
- ³ P. G. Blake, H. H. Davies, and G. Jackson, *J. Chem. Soc.* **1971**, 1923.
- ⁴ Y. N. Samsonov, A. K. Petrov, A. V. Baklanov, and V. V. Vihzin, *React. Kinet. Catal. Lett.* **5**, 197 (1976).
- ⁵ R. Corkum, C. Willis, and R. A. Back, *Chem. Phys.* **24**, 13 (1977).
- ⁶ D. K. Evans, R. D. McAlpine, and F. K. McClusky, *Chem. Phys.* **32**, 81 (1978).
- ⁷ D. S. Y. Hsu, W. M. Shaub, M. Blackburn, and M. C. Lin, *The Nineteenth International Symposium on Combustion* (The Combustion Institute, Pittsburgh, 1983), p. 89.
- ⁸ K. Saito, T. Kakamoto, H. Kuroda, S. Torii, and A. Imamura, *J. Chem. Phys.* **80**, 4989 (1984).
- ⁹ P. Ruelle, U. W. Kesselring, and H. Nam-Tran, *J. Am. Chem. Soc.* **108**, 371 (1986).
- ¹⁰ P. Ruelle, *J. Am. Chem. Soc.* **109**, 1722 (1987).
- ¹¹ P. Ruelle, *Chem. Phys.* **110**, 263 (1986).
- ¹² M. T. Nguyen and P. Ruelle, *Chem. Phys. Lett.* **138**, 486 (1987).
- ¹³ GAUSSIAN 86, M. J. Frisch, J. S. Binkley, D. J. DeFrees, K. Raghavachari, H. B. Schlegel, R. A. Whiteside, D. J. Fox, R. L. Martin, E. M. Fluder, C. F. Melius, L. R. Kahn, J. J. P. Stewart, F. W. Bobrowicz, and J. A. Pople, GAUSSIAN 86 (Carnegie-Mellon Quantum Chemistry Publishing Unit, Pittsburgh, 1984).
- ¹⁴ J. S. Binkley, J. A. Pople, and W. J. Hehre, *J. Am. Chem. Soc.* **102**, 939 (1980).
- ¹⁵ P. C. Hariharan and J. A. Pople, *Chem. Phys. Lett.* **66**, 217 (1972).
- ¹⁶ R. Krishnan, J. S. Binkley, R. Seeger, and J. A. Pople, *J. Chem. Phys.* **72**, 650 (1980).
- ¹⁷ J. S. Binkley and J. A. Pople, *J. Chem. Phys.* **66**, 879 (1977).
- ¹⁸ H. B. Schlegel, *J. Comput. Chem.* **3**, 214 (1982).
- ¹⁹ R. Krishnan and J. A. Pople, *Int. J. Quantum. Chem. Quantum Chem. Symp.* **14**, 91 (1980).
- ²⁰ J. A. Pople, H. B. Schlegel, R. Krishnan, D. J. DeFrees, J. S. Binkley, M. J. Frisch, R. A. Whiteside, R. F. Hout, and W. J. Hehre, *Int. J. Quantum Chem. S* **15**, 269 (1981).
- ²¹ R. G. Lerner, B. P. Dailey, and J. P. Friend, *J. Chem. Phys.* **26**, 680 (1957).
- ²² I. L. Karle and J. Karle, *J. Chem. Phys.* **22**, 43 (1954).
- ²³ A. D. McLean and Y. Ellinger, *Chem. Phys. Lett.* **98**, 450 (1983).
- ²⁴ M. S. Gordon, T. N. Truong, and J. A. Pople, *Chem. Phys. Lett.* **130**, 245 (1980).
- ²⁵ H. F. Schaefer, *Acc. Chem. Res.* **12**, 288 (1979).
- ²⁶ R. L. Redington, *J. Mol. Spectrosc.* **65**, 171 (1977).
- ²⁷ L. Radom, W. A. Lathan, W. J. Hehre, and J. A. Pople, *Aust. J. Chem.* **25**, 1601 (1972).
- ²⁸ M. R. Peterson and I. G. Csizmadia, *J. Am. Chem. Soc.* **101**, 1076 (1979).
- ²⁹ K. B. Wiberg and K. E. Laidig, *J. Am. Chem. Soc.* **109**, 5935 (1987).
- ³⁰ R. Fausto, L. A. E. Batistade deCarvalho, J. J. C. Teixeira-Dias, and M. N. Ramos, *J. Chem. Soc. Faraday Trans. 2* **85**, 9145 (1989).
- ³¹ T. Miyazawa and K. S. Pitzer, *J. Chem. Phys.* **30**, 1076 (1959).
- ³² D. L. Bernitt, K. O. Hartman, and I. C. Hisatsune, *J. Chem. Phys.* **42**, 3553 (1965).
- ³³ D. R. Lide, Jr., *Trans. Am. Crystallogr. Assoc.* **2**, 106 (1966).
- ³⁴ E. Bjarnov and W. H. Hocking, *Z. Naturforsch.* **330**, 610 (1978).
- ³⁵ J. D. Goddard, Y. Yamaguchi, and H. F. Schaefer III (to be published).
- ³⁶ D. Feller, W. T. Borden, and E. R. Davidson, *J. Chem. Phys.* **71**, 4987 (1979).
- ³⁷ D. Feller, W. T. Borden, and E. R. Davidson, *J. Comp. Chem.* **1**, 158 (1980).